JACS
JOURNAL OF THE AMERICAN CHEMICAL SOCIETY

Communication

pubs.acs.org/JACS

# Rational Design of Proteolytically Stable, Cell-Permeable Peptide-Based Selective Mcl-1 Inhibitors

Avinash Muppidi,[†] Kenichiro Doi,[‡] Selvakumar Edwardraja,[†] Eric J. Drake,[§] Andrew M. Gulick,[§] Hong-Gang Wang,[‡] and Qing Lin*,[†]

[†]Department of Chemistry, State University of New York at Buffalo, Buffalo, New York 14260-3000, United States

[‡]Department of Pharmacology, Pennsylvania State University College of Medicine, Hershey, Pennsylvania 17033, United States

[§]Hauptman-Woodward Institute and Department of Structural Biology, State University of New York at Buffalo, Buffalo, New York 14203, United States

Supporting Information

**ABSTRACT:** Direct chemical modifications provide a simple and effective means to "translate" bioactive helical peptides into potential therapeutics targeting intracellular protein−protein interactions. We previously showed that distance-matching bisaryl cross-linkers can reinforce peptide helices containing two cysteines at the *i* and *i*+7 positions and confer cell permeability to the cross-linked peptides. Here we report the first crystal structure of a biphenyl-cross-linked Noxa peptide in complex with its target Mcl-1 at 2.0 Å resolution. Guided by this structure, we remodeled the surface of this cross-linked peptide through side-chain substitution and N-methylation and obtained a pair of cross-linked peptides with substantially increased helicity, cell permeability, proteolytic stability, and cell-killing activity in Mcl-1-overexpressing U937 cells.

BH3-only proteins are pro-apoptotic factors that induce cell death through selective binding to anti-apoptotic Bcl-2 family proteins.[1] In a majority of cancers, interactions between pro-apoptotic BH3 proteins and anti-apoptotic Bcl-2 family proteins are deregulated because of elevated expression of some Bcl-2 family proteins such as Bcl-2, Bcl-$x_L$, and Mcl-1,[2] which contributes to cancer progression and renders cancer cells resistant to chemo- and radiotherapy.[3] A proven strategy in cancer therapeutic development is to design BH3 mimics as selective Bcl-2 inhibitors.[4] Two approaches have been successfully employed: (i) the use of small molecules to mimic BH3 peptide side chains involved in binding[5] and (ii) chemical modification of BH3 peptides to improve their pharmaceutical properties.[6] In the former approach, a potent small-molecule Bcl-2 inhibitor, ABT-737, was designed[7] that binds tightly to Bcl-2 and Bcl-$x_L$ with sub-nM affinity but poorly to Mcl-1;[8] in the latter, chemically modified BH3 peptides containing $\alpha/\beta$-amino acid backbones,[9] side-chain cross-linking,[10] and main-chain-to-side chain cross-linking[11] showed improved cell permeability and/or serum stability.

Mcl-1 is a member of the Bcl-2 family that undergoes frequent somatic amplification in multiple cancers and functions as a key driver of cancer cell survival.[12] Although small-molecule Bcl-2-selective inhibitors (e.g., ABT-263) have entered clinical trials, they generally lack efficacy in tumors with elevated levels of Mcl-1.[13] Since a NoxaB-(75−93)-C75A peptide derived from BH3-only Noxa protein binds to Mcl-1 with high affinity and selectivity,[14] an attractive approach for the development of Mcl-1-selective inhibitors is to optimize the pharmaceutical properties of Noxa BH3 peptide. We recently reported a new dicysteine alkylation-based side-chain cross-linking chemistry using a pair of distance-matching bisaryl cross-linkers that lead to reinforced peptide helices and improved cellular uptake.[15] Here we report the first crystal structure of a biphenyl-cross-linked Noxa BH3 peptide in complex with Mcl-1 and the subsequent design of a pair of proteolytically stable, cell-permeable, peptide-based Mcl-1 inhibitors by combining structure-based peptide side-chain cross-linking with peptide surface remodeling.

To apply our cysteine-mediated cross-linking chemistry to NoxaB-(75−93)-C75A peptide (hereafter called Noxa peptide), we replaced two solvent-exposed *i* and *i*+7 residues (Gln-77, Lys-84) in Noxa with D- or L-cysteine and subjected the 19-mer peptide to 4,4′-bis(bromomethyl)biphenyl (Bph)-mediated cross-linking (see Table S1 for peptide characterizations). The inhibitory activities of the cross-linked peptides were then evaluated using a competitive fluorescence polarization (FP) assay. Compared with the parent Noxa peptide, Bph-cross-linked peptides **1** and **2** showed 65- and 12-fold increases in inhibitory activity, respectively (Table 1). To verify that the Mcl-1 targeting selectivity remained intact after cysteine substitution and subsequent side-chain cross-linking, N-terminal fluorescein-conjugated, Bph-cross-linked Noxa peptides Fl-**1** and Fl-**2** were prepared, and their binding affinities toward Mcl-1 and Bcl-$x_L$ were measured using the FP assay. Gratifyingly, like Noxa, the cross-linked Noxa peptides showed comparable binding affinities toward Mcl-1 ($K_d$ = 4.9 ± 1.5 nM for Fl-**1**, 3.4 ± 0.2 nM for Fl-**2** vs 6.7 ± 1.0 nM for Noxa) but no measurable affinity toward Bcl-$x_L$ ($K_d$ > 1000 nM), indicating >200-fold selectivity for Mcl-1. As a control, the BH3 domain of the BH3-only protein Bim showed essentially equal potencies toward Mcl-1 and Bcl-$x_L$ in the same assay (Table S3). To our surprise, similar to the parent Noxa peptide, the cross-linked Noxa peptides **1** and **2** showed no activity in a cell viability assay in which Mcl-1-overexpressing U937 cells were treated with 20 $\mu$M peptide for 48 h, suggesting

**Received:** July 13, 2012
**Published:** August 25, 2012

**Table 1. Sequences and Biological Activities of the Native and Chemically Modified Noxa BH3 Peptides**

| Name | Sequence[a] | Charge | FP assay[b] $K_i$ (nM) | Cell viability[c] (%) |
|---|---|---|---|---|
| Noxa | AAQLRRIGDKVNLRQKLLN | +4 | 648±128 | 97.6±0.9 |
| **1** | AAC'LRRIGDC'VNLRQKLLN[d] | +3 | 10±1 | 98.6±4.0 |
| **2** | AAc'LRRIGDC'VNLRQKLLN[e] | +3 | 54±14 | 100.3±0.2 |
| **3** | AAc'LRAIGDC'VNLRQKLLN | +2 | 23±8 | 85.9±2.2 |
| **4** | AAc'LRAIGDC'VNLAQKLLN | +1 | 28±11 | 72.9±3.2 |
| **5** | AAc'LRAIGDC'VNLAQALLN | 0 | 29±4 | 44.3±0.2 |
| **6** | $A_m$Ac'LRRIGDC'VNLRQKLLN[f] | +3 | 32±3 | 87.3±2.8 |
| **7** | $A_mA_m$c'LRRIGDC'VNLRQKLLN | +3 | 22±4 | 80.5±4.7 |
| **8** | $A_mA_m$c'LRAIGDC'VNLAQALLN[g] | 0 | 22±8 | 34.8±0.5 |

[a]Peptides with N-terminal Ala were acetylated; those with N-terminal *N*-methylalanine were capped with methoxycarbonyl; all were amidated at the C-terminus. [b]Competitive FP assay performed three times to derive $K_i$ values and standard deviations. [c]Cell viability measured with ATP assay by treating Mcl-1-overexpressing U937 cells (cultured in RPMI1640 supplemented with 5% fetal bovine serum) with 20 $\mu$M peptide for 48 h. [d]C′ = Bph-linked L-cysteine. [e]c′ = Bph-linked D-cysteine. [f]$A_m$ = *N*-methylalanine. [g]Structure of **8**:

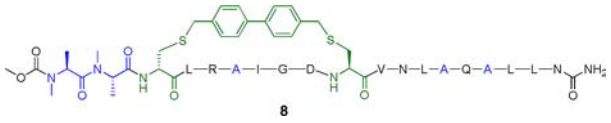


**8**

that Bph-mediated side-chain cross-linking is inefficient in allowing sufficient cytosolic transport.

To gain a structural understanding of how the cross-linked Noxa peptide binds to Mcl-1, we solved the crystal structure of mouse Mcl-1 (mMcl-1) in complex with **2** by molecular replacement. The structure was refined to 2.0 Å resolution with $R_{cryst}$ = 19.2% and $R_{free}$ = 23.9% (see Table S2 for crystal data and structural refinement). Overall, the Mcl-1 subunit in the complex is superimposable with the mMcl-1 NMR structure (PDB entry 2JM6) with a root-mean-square deviation of 1.2 Å (Figure S2).[14] Bound peptide **2** adopts a helical conformation, with the Bph cross-linker projecting 90° away from the deep hydrophobic binding groove (Figure 1a). Compared to 2JM6, most of the interactions between Noxa and mMcl-1 were maintained. A few H-bonds are formed only in the mMcl-1:**2** complex, namely, those between the Noxa Asp-9 and mMcl-1 Asn-241 side chains and between the Noxa Arg-5 side chain and the mMcl-1 backbone His-233 and Val-234. In addition, the Bph cross-linker forms an edge-to-face $\pi-\pi$ interaction with His-205 of mMcl-1 (Figure 1a). When cross-linked peptide **2** was superimposed with the linear Noxa peptide in 2JM6, significant changes in the side-chain orientations in **2** were observed for the solvent-exposed, positively charged residues (Figure 1b). For example, the Arg-6 side chain is disengaged from the salt bridge with Asp-238 of mMcl-1 and reoriented toward the Bph cross-linker; Arg-14 becomes completely solvent-exposed, as the salt bridge with the mMcl-1 Gly-308 carboxyl terminus was not detected; and the Lys-16 side chain is disengaged from the salt bridge with the Noxa Met-20 carboxyl terminus as a result of the Noxa peptide truncation. Together, the results suggest that these three solvent-exposed, positively charged residues can be replaced without loss of binding affinity toward Mcl-1.

Since molecules with large polar surface areas generally show poor passive membrane permeation,[16] we hypothesized that

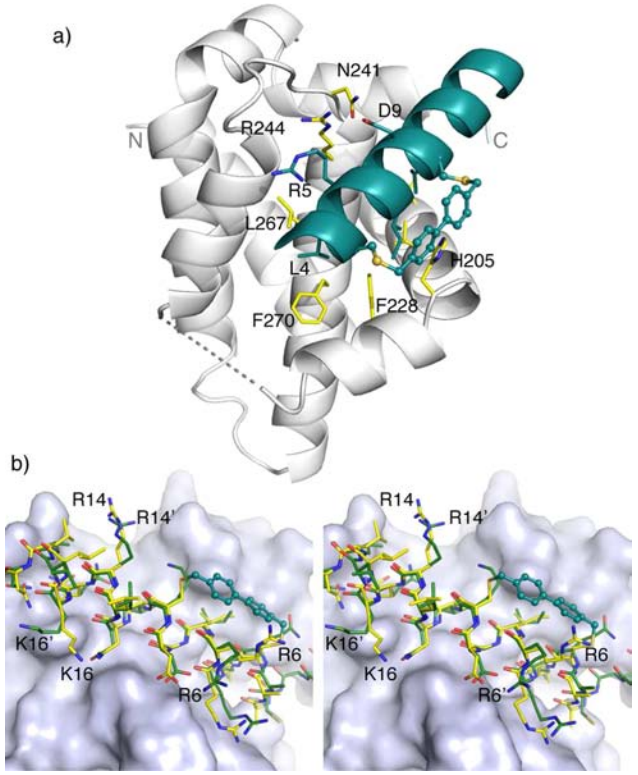


**Figure 1.** Crystal structure of mouse Mcl-1 in complex with Bph-cross-linked Noxa BH3 peptide **2**. (a) Overall complex structure. The peptide and the side chains of three canonical hydrophobic residues of peptide **2**, Leu-4 (h2), Ile-7 (h3), and Val-11 (h4), are colored in deep teal. The two flexible loops, Gly-173 to Gly-187 (in the front; shown as a dashed line) and Leu-216 to Val-224 (in the back; not shown), were disordered in the electron density maps. (b) Stereo view of superimposed Bph-cross-linked peptide **2** (yellow stick model) with mNoxa BH3 peptide (green stick model) as seen in 2JM6. The BH3-binding pocket of mMcl-1 is rendered as a surface model.

substituting the solvent-exposed charged residues with neutral ones would substantially improve the cell permeability of the cross-linked Noxa peptides, leading to increased cellular activity. Accordingly, we replaced one, two, or all three of the nonessential residues Arg-6, Arg-14, and Lys-16 in **2** with Ala to obtain cross-linked peptides **3**−**5**. We then assessed their inhibitory activities against Mcl-1 using competitive FP assay and their cell-killing activities in U937 cells using ATP assay (Table 1). To our satisfaction, a roughly 2-fold increase in inhibitory activity was observed after Ala substitution. More importantly, we observed progressive increases in cellular activity as the net charge decreased from +3 to 0, with only 44% of U937 cells remaining viable after treatment with charge-neutral cross-linked peptide **5** (20 $\mu$M). This implies that the charge-neutral peptide surface facilitates cytosolic transport of the cross-linked peptides, presumably through passive membrane diffusion. While **5** still has two charged residues, Arg-5 and Asp-9, which contribute to Mcl-1 binding (Figure 1a), it is tempting to speculate that they may form an internal salt bridge in the lipid bilayer during membrane transport because of their favorable *i*, *i*+4 geometry.

Encouraged by the initial Arg/Lys-to-Ala substitution results, we sought to further reduce the number of polar groups on the peptide surface to maximize passive membrane diffusion. In this regard, a proven modification is backbone N-methylation, especially for the N−H groups not involved in intramolecular H-bonding.[17] For the N-acyl-capped helical peptides, the first


dx.doi.org/10.1021/ja306864v | *J. Am. Chem. Soc.* 2012, 134, 14734−14737

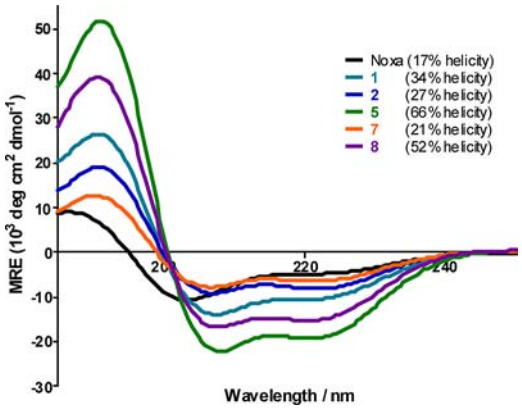


**Figure 2.** CD spectra of the Bph-cross-linked and linear Noxa peptides and their calculated percent helicities. The peptides were dissolved in 1:1 $CH_3CN/H_2O$ at a final concentration of 50 $\mu$M. The percent helicity was calculated using the $[\theta]_{222}$ value.

three N-terminal N−H groups typically are not engaged in intramolecular H-bonding because of the lack of preceding carbonyl groups one helical turn away. Careful examination of the structure of the Mcl-1:**2** complex reveals that the first two Ala N−H groups are solvent-exposed, while the third residue, D-Cys N−H, forms a H-bond with the capping acetyl group (H···O = 2.20 Å) (Figure S2c). We thus substituted one or both of the N-terminal alanines with *N*-methyl-Ala to generate the cross-linked peptides **6**−**8** and compared their inhibitory activities to that of their parent peptide (Table 1). We found that adding two *N*-methyl groups afforded higher activities in the FP and the cell viability assays (compare **7** to **2** and **8** to **5**). In particular, Bph-cross-linked peptide **8** containing two *N*-methyl groups in addition to three Ala substitutions showed the most robust activity in cell culture: only 35% of the U937 cells remained viable after treatment with **8** for 48 h (Table 1). A concentration-dependent ATP assay for **8** using U937 cells gave rise to a half-maximal effective concentration of 13.4 $\mu$M (Figure S3).

To probe the effect of chemical modifications on peptide secondary structure, we performed far-UV CD measurements and determined the helicities of cross-linked Noxa peptides **1**, **2**, **5**, **7**, and **8** along with the linear Noxa peptide (Figure 2). All of the Bph-cross-linked peptides had higher helicities than the linear Noxa peptide. Replacing the three positively charged residues with Ala in the cross-linked peptides led to a >2-fold increase in helicity (compare **5** to **2**), presumably as a result of the stronger helix-formation propensity of Ala relative to Arg and Lys.[18] Adding two *N*-methyl groups at the N-terminus appeared to destabilize the helix (compare **7** to **2**),[19] but the Ala-substituted, cross-linked peptide **8** seemed to tolerate N-methylation to some extent (52% helicity for **8** vs 66% for **5**).

To confirm that the increased cellular activity was a result of improved cytosolic transport, we prepared fluorescein-labeled Bph-cross-linked peptides Fluo-**2**, Fluo-**5**, and Fluo-**8**, together with Fluo-Noxa (Table S1). The uptake of these cross-linked and linear peptides into HeLa cells at 37 and 4 °C was analyzed by fluorescence-activated cell sorting. We expected the energy-dependent active transport processes (e.g., pinocytosis, previously reported to be a major membrane permeation pathway for side-chain cross-linked peptides[20]) to be inhibited at 4 °C and the passive membrane diffusion to remain unaffected. Not surprisingly, we observed that Bph-mediated cross-linking enhanced peptide cellular uptake 26−40-fold at 37 °C and 7−33-fold at 4 °C (compare Fluo-**2**, -**5**, and -**8** to Fluo-Noxa in Figure 3b,c). However, the effect of the temperature switch from 37 to 4 °C varied: the +3 charged, cross-linked peptide **2** showed 82% reduction, whereas the Ala-substituted, charge-neutral cross-linked peptides showed much smaller reductions (48% for Fluo-**5** and 45% for Fluo-**8**). The dramatic reduction in cellular uptake of Fluo-**2** indicates that **2** permeates into cells mainly through the energy-dependent endocytotic process, resulting in endosome trapping. The smaller reductions for **5** and **8** indicate that passive membrane diffusion represents a major pathway for the uptake because of their favorable physicochemical properties, including neutral charge, reduced number of polar groups on their surfaces, and overall higher helicity. A confocal microscopy experiment confirmed that the cross-linked peptides **5** and **8** were predominantly localized in the cytosol and not bound to the cell membrane (Figure S4).

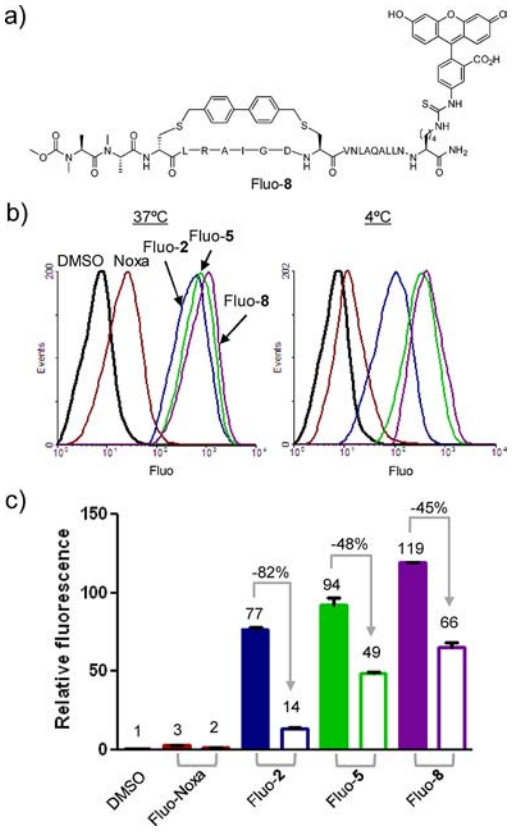


**Figure 3.** Flow cytometry analysis of HeLa cells after treatment with Fluo-Noxa, Fluo-**2**, Fluo-**5**, and Fluo-**8** (10 $\mu$M). (a) Structure of Fluo-**8**. (b) Representative flow cytometry histograms at 37 °C (left) and 4 °C (right). (c) Bar graph showing normalized relative fluorescence at 37 °C (filled) and 4 °C (open).

A key benefit of peptide side-chain cross-linking is improved proteolytic stability. To test this, we selected the most potent Bph-cross-linked peptides, **5** and **8**, and compared their proteolytic stabilities to that of the parent Noxa peptide in the presence of chymotrypsin, trypsin, and mouse serum (Figure 4). In all three cases, **5** and **8** exhibited greatly improved proteolytic stabilities relative to the linear Noxa peptide: 8.7- and 7.2-fold improvements in half-life ($t_{1/2}$) against chymotrypsin and 14.8- and 8.9-fold improvements against trypsin, respectively. The higher stability of **5** relative to **8** can be attributed to its higher helicity (66% vs 52%). The most dramatic effect was seen with mouse serum, where the linear Noxa peptide showed a $t_{1/2}$ of only 10.5 ± 2.3 min, while for **5** and **8** $t_{1/2}$ = 31.6 ± 2.2 and 21.2 ±


dx.doi.org/10.1021/ja306864v | J. Am. Chem. Soc. 2012, 134, 14734−14737

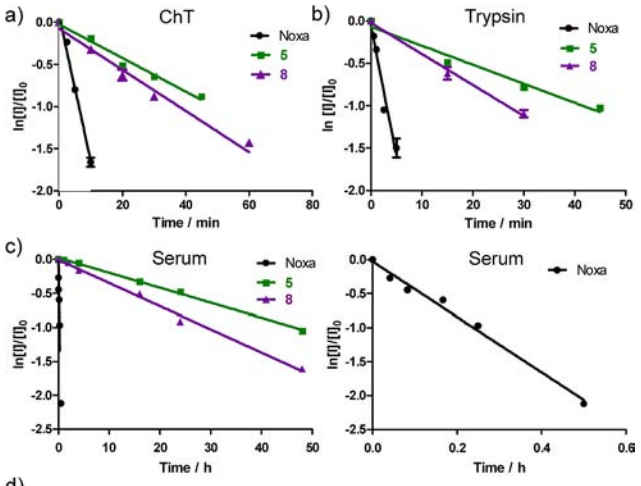


d)

| | $t_{1/2}$ (ChT) | $t_{1/2}$ (trypsin) | $t_{1/2}$ (serum) |
|---|---|---|---|
| Noxa | 4.1 ± 0.5 min | 2.2 ± 0.3 min | 10.5 ± 2.3 min |
| **5** | 35.5± 4.5 min | 32.5± 5.5 min | 31.6 ± 2.2 h |
| **8** | 29.7± 5.0 min | 19.6± 3.5 min | 21.2 ± 2.6 h |

**Figure 4.** Proteolytic stabilities of the linear and Bph-cross-linked Noxa peptides in the presence of (a) chymotrypsin (ChT), (b) trypsin, and (c) mouse serum (with a zoom-in of the degradation plot for the linear Noxa peptide shown on the right). (d) Calculated average $t_{1/2}$ values for the peptides. The measurements were performed three times for ChT and trypsin and twice for mouse serum.

2.6 h, representing 180- and 121-fold increases in stability, respectively. This prolonged stability may also be partly due to the presence of the hydrophobic biphenyl cross-linker in **5** and **8**, which facilitates sequestration/protection of the Bph-cross-linked peptides by serum albumin proteins.[21]

In conclusion, we have solved the first crystal structure of a biphenyl-cross-linked peptide in complex with its target Mcl-1. Similar to the crystal structures involving hydrocarbon cross-linkers,[22] the biphenyl cross-linker formed an edge-to-face $\pi-\pi$ interaction with His-205 of Mcl-1, potentially contributing to tighter binding. Using the structural insights we obtained, we successfully remodeled the surface of the cross-linked peptide through residue substitution and backbone N-methylation and obtained a pair of cross-linked peptides with greatly increased helicity, cell permeability, proteolytic stability, and cell-killing activity in Mcl-1-overexpressing cancer cells. While side-chain cross-linking has become a major strategy for translating bioactive helical peptides into potential therapeutics targeting intracellular protein−protein interactions,[23] the work presented here illustrates the subtlety of each system and highlights the value of complementary peptide modification chemistries (e.g., N-methylation).

## ■ ASSOCIATED CONTENT

### Ⓢ Supporting Information

Experimental details and characterization data; complete refs 2c, 6, 12, 14, and 17. This material is available free of charge via the Internet at http://pubs.acs.org. The crystal structure of Mcl-1 in complex with **2** has been deposited in the Protein Data Bank as entry 4G35.

## ■ AUTHOR INFORMATION

### Corresponding Author

qinglin@buffalo.edu

### Notes

The authors declare no competing financial interest.

## ■ ACKNOWLEDGMENTS

We gratefully acknowledge the Pardee Foundation and the Oishei Foundation (to Q.L.) and the National Institutes of Health (CA82197 to H.-G.W.; GM068440 to A.M.G.) for financial support.

## ■ REFERENCES

(1) (a) Willis, S. N.; Adams, J. M. *Curr. Opin. Cell Biol.* **2005**, *17*, 617. (b) Chen, L.; Willis, S. N.; Wei, A.; Smith, B. J.; Fletcher, J. I.; Hinds, M. G.; Colman, P. M.; Day, C. L.; Adams, J. M.; Huang, D. C. *Mol. Cell* **2005**, *17*, 393.

(2) (a) Vaux, D. L.; Cory, S.; Adams, J. M. *Nature* **1988**, *335*, 440. (b) Minn, A. J.; Rudin, C. M.; Boise, L. H.; Thompson, C. B. *Blood* **1995**, *86*, 1903. (c) Beroukhim, R.; et al. *Nature* **2010**, *463*, 899.

(3) Reed, J. C. *Adv. Pharmacol.* **1997**, *41*, 501.

(4) (a) Lessene, G.; Czabotar, P. E.; Collman, P. M. *Nat. Rev. Drug Discovery* **2008**, *7*, 989. (b) Chonghaile, T. N.; Letai, A. *Oncogene* **2009**, *27*, S149.

(5) (a) Kutzki, O.; Park, H. S.; Ernst, J. T.; Orner, B. P.; Yin, H.; Hamilton, A. D. *J. Am. Chem. Soc.* **2002**, *124*, 11838. (b) Yin, H.; Lee, G. I.; Sedey, K. A.; Kutzki, O.; Park, H. S.; Orner, B. P.; Ernst, J. T.; Wang, H. G.; Sebti, S. M.; Hamilton, A. D. *J. Am. Chem. Soc.* **2005**, *127*, 10191.

(6) Oltersdorf, T.; et al. *Nature* **2005**, *435*, 677.

(7) van Delft, M. F.; Wei, A. H.; Mason, K. D.; Vandenberg, C. J.; Chen, L.; Czabotar, P. E.; Willis, S. N.; Scott, C. L.; Day, C. L.; Cory, S.; Adams, J. M.; Roberts, A. W.; Huang, D. C. *Cancer Cell* **2006**, *10*, 389.

(8) Tahir, S. K.; Wass, J.; Joseph, M. K.; Devanarayan, V.; Hessler, P.; Zhang, H.; Elmore, S. W.; Kroeger, P. E.; Tse, C.; Rosenberg, S. H.; Anderson, M. G. *Mol. Cancer Ther.* **2010**, *9*, 545.

(9) Horne, W. S.; Boersma, M. D.; Windsor, M. A.; Gellman, S. H. *Angew. Chem., Int. Ed.* **2008**, *47*, 2853.

(10) (a) Walensky, L, D.; Kung, A. L.; Escher, I.; Malia, T. J.; Barbuto, S.; Wright, R. D.; Wagner, G.; Verdine, G. L.; Korsmeyer, S. J. *Science* **2004**, *305*, 1466. (b) Walensky, L. D.; Pitter, K.; Morash, J.; Oh, K. J.; Barbuto, S.; Fisher, J.; Smith, E.; Verdine, G. L.; Korsmeyer, S. J. *Mol. Cell* **2006**, *24*, 199.

(11) Wang, D.; Liao, W.; Arora, P. S. *Angew. Chem., Int. Ed.* **2005**, *44*, 6525.

(12) (a) Inuzuka, H.; et al. *Nature* **2011**, *471*, 104. (b) Wertz, I. E.; et al. *Nature* **2011**, *471*, 110.

(13) (a) Lin, X.; Morgan-Lappe, S.; Huang, X.; Li, L.; Zakula, D. M.; Vernetti, L. A.; Fesik, S. W.; Shen, Y. *Oncogene* **2007**, *26*, 3972. (b) Yecies, D.; Carlson, N. E.; Deng, J.; Letai, A. *Blood* **2010**, *115*, 3304.

(14) Czabotar, P. E.; et al. *Proc. Natl. Acad. Sci. U.S.A.* **2007**, *104*, 6217.

(15) Muppidi, A.; Wang, Z.; Li, X.; Chen, J.; Lin, Q. *Chem. Commun.* **2011**, *47*, 9396.

(16) Refsgaard, H. H.; Jensen, B. F.; Brockhoff, P. B.; Padkjar, S. B.; Guldbrandt, M.; Christensen, M. S. *J. Med. Chem.* **2005**, *48*, 805.

(17) (a) Biron, E.; et al. *Angew. Chem., Int. Ed.* **2008**, *47*, 2595. (b) White, T. R.; et al. *Nat. Chem. Biol.* **2011**, *7*, 810.

(18) Pace, C. N.; Scholtz, J. M. *Biophys. J.* **1998**, *75*, 422.

(19) Chang, C. F.; Zehfus, M. H. *Biopolymers* **1996**, *40*, 609.

(20) (a) Bird, G. H.; Bernal, F.; Pitter, K.; Walensky, L. D. *Methods Enzymol.* **2008**, *446*, 369. (b) Madden, M. M.; Rivera Vera, C. I.; Song, W.; Lin, Q. *Chem. Commun.* **2009**, 5588.

(21) Specific binding of Fluo-**8** to homologous BSA at protein concentrations as low as 25 $\mu$g/mL was detected by direct FP assay (see Figure S5).

(22) (a) Stewart, M. L.; Fire, E.; Keating, A. E.; Walensky, L. D. *Nat. Chem. Biol.* **2010**, *6*, 595. (b) Baek, S.; Kutchukian, P. S.; Verdine, G. L.; Huber, R.; Holak, T. A.; Lee, K. W.; Popowicz, G. M. *J. Am. Chem. Soc.* **2012**, *134*, 103.

(23) Verdine, G. L.; Walensky, L. D. *Clin. Cancer Res.* **2007**, *13*, 7264.